ACS Sustainable Chemistry & Engineering

pubs.acs.org/journal/ascecg

Research Article

Biorefining of Thermoplastic Starch via Depolymerization and Methane Arrested Anaerobic Digestion

Published as part of ACS Sustainable Chemistry & Engineering special issue "Advancing a Circular Economy".

Weishen Zeng, Kasper D. de Leeuw, and David P. B. T. B. Strik*

Cite This: *ACS Sustainable Chem. Eng.* 2025, 13, 8116–8127

Read Online

ACCESS | Metrics & More | Article Recommendations | Supporting Information

ABSTRACT: In the circular plastics economy, biodegradable plastic waste streams become a resource to be recycled with thoughtful integration of physiochemical and microbial processes. Anaerobic digestion as well as the carboxylate platform provide opportunities to convert complex biomass, including biodegradable plastic waste. Here, we study how a commercial thermoplastic starch (TPS) product, which typically displays poor digestibility into biogas, can be biorefined into various chemicals. First, abiotic depolymerization was studied under mesophilic (35 °C) and thermophilic conditions (55 and 70 °C) over 56 days. The results showed accelerated hydrolysis and microplastic formation at higher temperatures, impacting the TPS morphology and disintegration process. TPS material characterization revealed the presence of PBAT (polybutylene adipate-*co*-terephthalate) and PLA (polylactic acid) as copolymers. The highest hydrolysis efficiency was 36.3%, with glucose, lactic acid (LA), terephthalic acid (TPA), adipic acid (AA), and 1,4-butanediol (1,4-BDO) identified. Besides abiotic treatment, methane-arrested anaerobic digestion of solid TPS and/or hydrolysates was studied within 14 days. Hereby, up to 23.1% of the provided materials was converted into volatile fatty acids. Consumption of glucose and lactate suggests that anaerobic biological conversion including microbial chain elongation occurred, while 1,4-BDO, AA, and TPA were unconverted. With these findings, a biorefinery concept was developed to recover chemicals from TPS-containing waste streams.

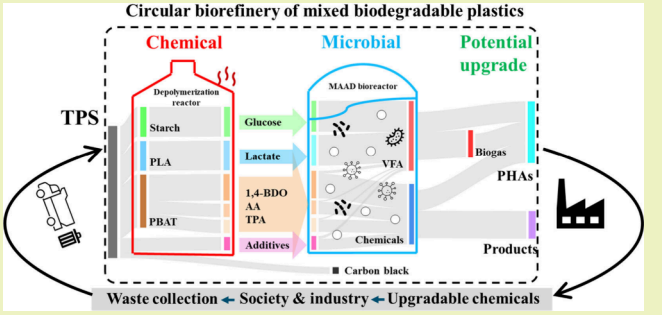

KEYWORDS: *Bioplastic, microbial recycling, agricultural mulch film, mixed-culture fermentation, VFA platform, chain elongation, carboxylates, polyhydroxyalkanoates*

1. INTRODUCTION

The transition to a circular plastic economy is seen as an indispensable part of establishing a sustainable society.[1,2] This includes the appeal to gradually move from fossil-based plastics toward biobased, CO_2-based, and circular-based plastics.[3] The European Commission has formulated a circular plastic economy strategy to facilitate circular plastic production and drive innovative recycling solutions that reduce plastic waste and keep materials in the loop.[4] Corresponding to this is the ongoing establishment of the United Nations plastic treaty, which aims to develop a legally binding international instrument to address plastic pollution across its entire lifecycle.[5] Such developments align with the vision to move away from nonbiodegradable plastics to biodegradable plastics and develop lower carbon footprint materials.[6,7] However, biodegradable plastics should be carefully formulated, used, and disposed of to effectively utilize the specific intrinsic biodegradability properties of its constituents and reduce its environmental impact.[8]

Nowadays, biodegradable plastics are increasingly produced, reaching 1.1 million tons in 2023, and scenarios predict a 4.6 million ton annual production in 2028.[9] Thermoplastic starch (TPS) is one of the top 3 most used materials in biodegradable plastic products globally in 2024, with a share of 5.7%. The other two are polylactic acid (PLA, 37.1%) and poly(butylene adipate-*co*-terephthalate) (PBAT, 4.6%).[9] TPS is widely applied in agriculture as mulch film and packaging in the form of bags.[10] The end-of-life practices of biodegradable plastics like TPS are poorly quantified.[11] Plastic-containing waste streams, which may contain TPS, follow practices such as landfilling, composting, anaerobic digestion, and/or incineration but are also unintentionally spilled into the

Received: March 15, 2025
Revised: April 29, 2025
Accepted: April 30, 2025
Published: May 16, 2025

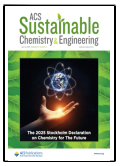

Table 1. Experimental Plans for TPS Mulch Film Hydrolysis and Anaerobic Fermentation[a]

Hydrolysis of TPS Mulch Film					Fermentation of Hydrolyzed TPS			
Label	Mulch Film (g)	Temperature (°C)	0.2 M PBS (mL)	Demineralized Water (mL)	Label	Original TPS (g COD)	Liquid Fraction (g COD)	Solid Fraction (g COD)
PB35	8.0	35	20	80	Blank			
CH35	8.0	35		100	TF	10		
PB55	8.0	55	20	80	LF		10	
CH55	8.0	55		100	SF			10
PB70	8.0	70	20	80	LSF		5	5
CH70	8.0	70		100				

[a]Note: PB35, PB55, and PB70 refer to experiments conducted with phosphate buffer solution and demineralized water as the medium at 35 °C, 55 °C, and 70 °C, respectively. CH35, CH55, and CH70 indicate experiments with only demineralized water in the medium at 35 °C, 55 °C, and 70 °C, respectively. TF represents the fermentation of the original TPS fraction. LF represents the fermentation of the liquid fraction of CH70. SF represents the fermentation of the solid fraction of CH70. LSF represents the fermentation of the combined liquid and solid fractions of CH70.

environment.[12] Moreover, TPS products are specifically designed to degrade in the field, as is the case with agricultural mulch films. These established end-of-life practices will typically result in (partial) degradation of the TPS materials, whereby its carbon is emitted as CO_2 into the air. This dilute CO_2 gas can again be used to grow plants as a bioresource for new biodegradable plastic compounds present in TPS.[3] However, the effectiveness of this method of carbon recycling can be debated since one has to construct a whole new material again from starch, accompanied by land, energy, nutrients, water, and other resource needs.[13,14] Various studies report on using biodegradable plastic waste and reproducing new bioplastics or other materials in more direct ways by rethinking the end-of-life of biodegradable products.[15−17] Once recycling processes that retain unoxidized carbon within the materials loop are established and virgin plastics are produced from biomass or CO_2, the overall plastic system can conceptually become carbon-negative, helping to mitigate the problems caused by the large-scale release of fossil-based CO_2.[7]

Microbial plastic biorecycling processes use living microorganisms as biocatalysts.[18,19] TPS products, like biowaste bags, are entering anaerobic digestion facilities, wherein they may be largely converted into methane-rich biogas.[11,17] Anaerobic digestion is an open-culture bioprocess wherein distinct functional groups of microorganisms break down complex feedstock, typically forming volatile fatty acids (VFAs) as intermediates, into the gaseous chemicals like methane and CO_2.[20] According to the World Biogas Association's estimation, around 132,000 small, medium, or large-scale digesters are operating worldwide.[21] These widely available digesters typically treat a plurality of biowaste materials including TPS and several other types of biodegradable plastics. The derived biogas is often valorized for heat and power production or upgraded to transport fuel.[21] The methane can potentially be used as feedstock to make new biodegradable plastics by microorganisms in the form of polyhydroxyalkanoates (PHA);[22,23] however, this would be cumbersome. Alternatively, the digestion process can be halted at the VFA intermediates, allowing for the carboxylates to be valorized.

The anaerobic digestibility of TPS materials depends on the composition of the material and both physicochemical and fermentation conditions. Narancic et al. described 98% and 80% degradation percentages of starch-rich TPS material (85% of starch) following standardized methods via aquatic anaerobic digestion (35 °C) and high-solids anaerobic digestion (52 °C), respectively.[8,24] However, commercial TPS products generally display a relatively poorer bioconversion degree than starch-rich polymers, likely because they contain more hydrophobic copolymers and additives in order to improve the mechanical properties and water resistance of TPS.[25,26] These material complexities can cause unpredictable degradation behaviors and challenges for biodegradable plastic digestion processes.[26−28]

So far, no studies have been available that look into the anaerobic fermentation of TPS under so-called methane-arrested anaerobic digestion (MAAD) conditions.[29] In the presence of exogenous biological inhibitors or unfavorable conditions for methanogen growth, the anaerobic digestion process can shift toward a VFA production process.[30] TPS does contains starch, which is a known precursor for VFA, ethanol, or lactate production.[31] Therefore, TPS is hypothetically under MAAD conditions fermentable into VFA. Once specific substrates that favor the microbial chain elongation process (like ethanol) are available, then medium-chain fatty acids (MCFAs) and corresponding alcohols can also be produced.[32] These carboxylates are value-added chemicals that can also be used to produce PHA bioplastics or serve other applications as described in the so-called VFA or carboxylate platform.[33,34] TPS has been well studied for biogas formation, but how the conversion of various TPS compounds occurs is not revealed. Insights on the material properties and the chemicals formed during depolymerization and anaerobic fermentation of TPS can help to better understand how to deal with TPS-based products at their end-of-life.

The objective of this study was to reveal the depolymerization processes and characterize the anaerobic digestion of TPS and its hydrolysates under methane-inhibited conditions. As study material, a commercially available TPS mulch film containing Mater-Bi was purchased. First, the TPS material was hydrolyzed at mesophilic (35 °C) and thermophilic (55 and 70 °C) temperatures with the medium being either demineralized water or phosphate buffer solution (PBS). Meanwhile, Fourier transform infrared (FT-IR) and X-ray diffraction (XRD) were used to identify the components of the TPS mulch film. Hereafter, the hydrolysates of the 70 °C experiment (which yielded the highest soluble chemical oxygen demand), the solid TPS residues, mixtures thereof, and the original TPS were submitted to MAAD to explore the extent of VFA production from the polymer and its constituents. The study provides insights into how various microbial recycling routes can be aggregated into a biorefinery concept to recover chemicals from TPS-containing waste streams.

https://doi.org/10.1021/acssuschemeng.5c02366
ACS Sustainable Chem. Eng. 2025, 13, 8116−8127

2. MATERIALS AND METHODS

2.1. Materials and Reagents. A commercially available thermoplastic starch (TPS) mulch film,[35] certified to meet EN 17033 standards,[36] was obtained. According to the manufacturer's specifications, the mulch film contains corn/potato starch, vegetable oil, and Mater-Bi.[37] The total chemical oxygen demand (COD) of the mulch film was determined to be 1.71 ± 0.03 g COD/g mulch film.

In the TPS mulch film hydrolysis experiments, a 0.2 mol/L phosphate buffer solution (PBS) at pH 7.0, prepared from $Na_2HPO_4 \cdot 2H_2O$ and KH_2PO_4, was employed. Sodium L-lactate (99%, Merck), 1,4-butanediol (ReagentPlus, 99% purity, Merck), adipic acid (≥99.5% purity, Merck), and terephthalic acid (>98% purity, Merck) were used as standards to assess the composition of the hydrolyzed TPS.

For the methane-arrested anaerobic digestion experiments, a bacterial culture medium was used as the nutrient source, comprising macronutrients (20 mL/L), trace elements (0.5 mL/L), and vitamins (1 mL/L).[38] To inhibit methane (CH_4) production, 5 g/L 2-bromoethanesulfonate (BES) was added to the medium. BES is a well-known methane inhibitor, functioning as a coenzyme M analogue that directly inhibits the methanogenesis pathway.[39] Additional details regarding the medium composition are provided in the Supporting Information.

2.2. Methodology. *2.2.1. TPS Hydrolysis Experiments.* Batch serum flask hydrolysis experiments of TPS mulch film were conducted, as outlined in Table 1. Each 250 mL serum flask had a working volume of 100 mL and contained 8.01 ± 0.01 g of TPS mulch film, cut into approximately 2 × 2 cm square pieces, with either PBS or demineralized water added. The flasks were sealed with rubber stoppers and aluminum caps, leaving a headspace of approximately 150 mL of air. Flasks were labeled, covered with aluminum foil, and placed in temperature-controlled shakers to maintain mesophilic (35 °C), low-thermophilic (55 °C), and high-thermophilic (70 °C) conditions. Liquid samples (2 mL) were collected for analysis three times during the first 2 weeks and then once per week after that. Sampling was performed using a 2 mL syringe, primarily drawn from the liquid fraction, with minimal removal of visible solid material. At the end of the hydrolysis experiments, the hydrolyzed TPS was separated into liquid and solid fractions by settling, allowing for the determination of their chemical composition and properties.

2.2.2. Anaerobic Fermentation Experiments. Hydrolyzed TPS anaerobic fermentation experiments were carried out in batch serum flasks following hydrolysis (Table 1). Hydrolyzed TPS mulch film (CH70) demonstrated the highest hydrolysis performance and was selected as the research focus. CH70 was separated into solid and liquid fractions to evaluate its potential for VFA production under MAAD conditions. Batch fermentation was inoculated with a mixture of two inocula: one from a glucose-based chain elongation reactor (Wageningen University and Research, Environmental Technology) and the other from cow rumen fluid (Wageningen University and Research, Animal Sciences). The total COD was set at 10 g of COD/L, and macronutrients, trace elements, and vitamins were added to ensure sufficient nutrients for microbial growth. The pH was adjusted to 7 before the flasks were sealed with rubber stoppers and aluminum caps. Inoculum was added at 2% (v/v), and the headspace was flushed with a CO_2/N_2 mixture (20%/80%) for 15 min to achieve a pressure of 1.5 bar. Fermentation was carried out in a temperature-controlled shaker at 35 °C and 150 rpm for 14 days, with each experimental group performed in triplicate. During fermentation, pH, soluble chemical oxygen demand (SCOD), VFA, and concentration of TPS monomers were analyzed.

2.3. Characterization and Analytical and Calculations Methods. *2.3.1. Particle Size Distribution.* The particle size distribution of hydrolyzed TPS (PB70 and CH70) was determined by using a laser diffraction particle size analyzer (Shimadzu, SLAD-2300). The measurement range was from 0.017 to 2500 μm. Before measurement, the solid fractions of PB70 and CH70 were further separated by a 1 mm sieve because some plastic particles were bigger than the analyzer's maximum size (2500 μm). For more details, see the Supporting Information (Table S2). The dispersant was demineralized water. The absorption index was set to 0.01, and the refractive indices of TPS were set to 1.500.[40] Each sample was measured three times.

2.3.2. Light and Scanning Electron Microscope (SEM) Imaging. Surface morphological characteristics of TPS mulch film and fermented solid samples were observed by a microscope (Nikon, Eclipse E400) and scanning electron microscope (FEI Magellan 400). Fermented TPS (TF, SF, LSF) immediately fixed in 2.5% glutaraldehyde with 0.2 M phosphate buffer solution for 4 h at room temperature after fermentation. Then, samples were washed six times with phosphate buffer solution and dehydrated with a series of ethanol solutions (30%, 50%, 70%, 90%, and 95% for 15 min and 100% for 45 min).[41] After that, samples were dried at 35 °C for 24 h and covered by thin (0.5−20 nm) gold conducting layers via sputter coating. Then, samples were analyzed by SEM with an electron energy range from 1 to 30 kV and a subnanometer resolution (0.8 nm at 15 kV, 0.9 nm at 1 kV). Meanwhile, the disintegration and hydrolysis processes of the TPS mulch film were tracked by mobile phone cameras for up to 56 days.

2.3.3. Fourier Transform Infrared (FT-IR) and X-ray Diffraction (XRD) of TPS. To analyze the change of functional groups in the TPS mulch film, we analyzed the residues by FT-IR (Bruker, ALPHA II) at the wavenumber of 400−4000 cm^{-1}. XRD analysis was carried out by using an X-ray powder diffractometer (Bruker) at a scan rate of 6°/min from 5° to 30° to determine the crystal structure of the original and hydrolyzed TPS. Accelerating voltage and current were 40 kV and 40 mA, respectively. The crystallinity of TPS was analyzed by DIFFRAC software (Bruker, Version 5.2).

2.3.4. Liquid and Gas Composition Analysis. All liquid samples were centrifuged at 15 000 rpm for 10 min before measurement. The total COD of the TPS mulch film and SCOD were determined by LCK 514 kits (HACH GmbH, Germany) after filtration with a 0.45 μm filter. pH was measured by a pH meter (PHM210, MeterLab). VFA and ethanol were quantified using gas chromatography (GC, Agilent 7890B) after pretreating the samples with 15% formic acid to lower the pH. In contrast, 1,4-butanediol (1,4-BDO) was measured using the same GC system without acidification. Lactic acid (LA) was measured by high-performance liquid chromatography (HPLC, Dionex Ultimate 3000). Adipic acid (AA) was also measured by HPLC (Waters, ACQUITY UPLC H-Class PLUS System), which is equipped with an ultraviolet (UV) detector and a Refractive Index (RI) detector. A 15 cm × 4.6 mm Rezex ROA-Organic Acid H^+ (8%) column with a prefilter was used. All samples were acidified by 5 mM H_2SO_4 and 9% of acetonitrile. In this HPLC method, the lactate peak was positioned adjacent to the adipate peak, with a slight overlap. This overlap may have caused a reduction in the integral area of the adipate peak. Terephthalic acid (TPA) was measured by ultraviolet−visible spectrophotometry (Tecan, infinite M200 pro) at 240 nm.[42] 0.100 g of pure TPA was dissolved in 25 mL of NaOH (1 M) and then diluted into a series of TPA standard solutions (0.000 mg/mL, 0.004 mg/mL, 0.008 mg/mL, 0.012 mg/mL, 0.016 mg/mL, 0.020 mg/mL). Samples were diluted with only demineralized water.

Before fermentation liquid samples were collected, the headspace pressure was measured using a gas pressure meter (Greisinger, GMH 3151). The gas composition of the headspace, including N_2, CO_2, O_2, and CH_4, was analyzed using gas chromatography (GC, Shimadzu 2010).[38,43]

2.4. Calculations and Statistical Analyses. All data was analyzed by Excel. All figures were drawn by ORIGIN software (Version 2024b). The error bars in the figures represent the standard deviation. The hydrolysis efficiency of TPS and VFA yield was statistically analyzed via standard deviation using One-way ANOVA (SPSS, Version 28.0.1.1). The mean difference is significant at the 0.05 level. The hydrolysis efficiency was determined based on soluble COD measurements and calculated as follows:

https://doi.org/10.1021/acssuschemeng.5c02366
ACS Sustainable Chem. Eng. 2025, 13, 8116−8127

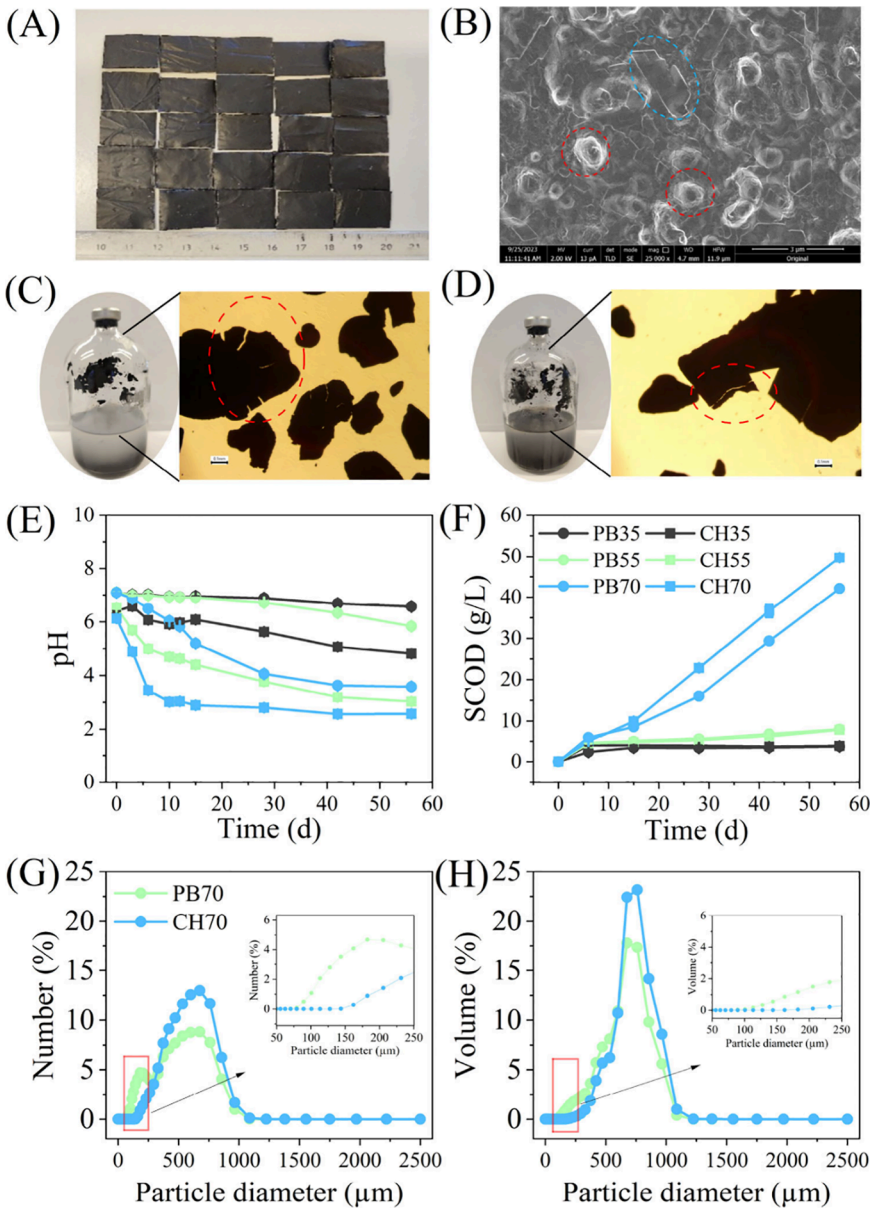

Figure 1. (A) Original TPS mulch film material studied cut into 2 × 2 cm pieces before hydrolysis. (B) SEM image of original TPS mulch film (magnification 25 000×; red circles may represent starch, and blue circle may represent copolymers). (C, D) Microscopic images of constituents of PB70 and CH70 at day 56. (E, F) The change of pH and SCOD concentration during TPS hydrolysis experiments at different temperatures (35, 55, and 70 °C) with phosphate buffer (PB) or with demineralized water (CH); error bars represent the standard deviation; (G, H) Exemplary particle size distributions of microplastics formed from TPS degradation at 70 °C.

$$\text{Hydrolysis efficiency (\%)} = \frac{\text{Soluble COD of hydrolysate}}{\text{Total COD of TPS}} \times 100\%$$

3. RESULTS AND DISCUSSION

3.1. TPS Disintegration and Hydrolysis Accelerate with Higher Temperatures and Lead to Microplastic Formation. Microbial degradation of biodegradable plastic typically follows fragmentation, leaching, and/or hydrolysis into soluble particulate before assimilation by microorganisms occurs.[44] Biodegradable mulch films have proven to be at least partially biodegraded in soil field conditions.[45,46] The present work first studied the TPS material characteristics, degradation, and depolymerization behavior under intended abiotic conditions within a buffered and pure demineralized water medium. From SEM images (Figure 1B), it was observed that the studied TPS mulch film contains spherical granules, which is likely attributed to starch as the previous study shows,[47] but some irregular square and net structures were also found. This means that the TPS mulch film product has a heterogeneous morphology, which may lead to spatially irregular disintegration and hydrolysis due to different local material properties.

The different applied temperatures affected the disintegration and hydrolysis processes of the TPS. Looking at images taken during the experiments (Figure S1), it is evident that disintegration occurs most rapidly at 70 °C (PB70 and CH70) and second at 55 °C (PB55 and CH55). At 70 °C, TPS rapidly started to fragment within 10 days and kept fragmenting until the experiment was stopped. While looking at light microscope

https://doi.org/10.1021/acssuschemeng.5c02366
ACS Sustainable Chem. Eng. 2025, 13, 8116−8127

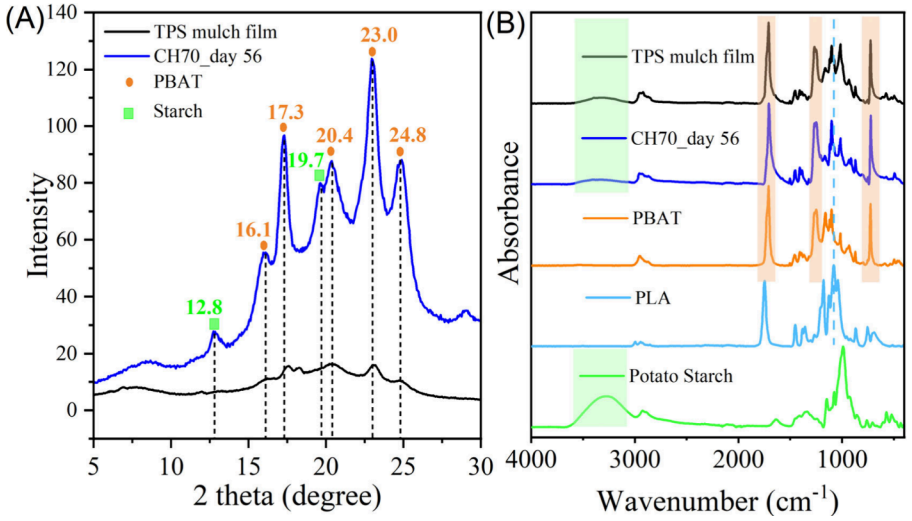

Figure 2. XRD and FTIR patterns of the original TPS mulch film, the solid residues after hydrolysis at 70 °C, and the standard spectra of PBAT, starch, and PLA. Highlighted peaks/areas are explained in the text.

images of PB70 and CH70 (Figure 1C,D), it was found that TPS mulch film, as expected, cracks irregularly during disintegration processes. PB55 and CH55 experiments showed the clear fragmentation of plastic squares into thin fibers after 28 days. At 35 °C, the TPS hardly disintegrated within 56 days. Here, it was visible by the eye that large square plastic parts were still present at the end of the hydrolysis experiment. The total of hydrolysate was measured as the soluble chemical oxygen demand. Here, an upward tendency with a significant difference between low and high applied temperatures was shown (Figure 1F). The SCOD of PB35 and CH35 slowly increased before stabilizing at 3.74 ± 0.08 g/L and 3.87 ± 0.05 g/L, respectively, after 14 days. The SCOD of PB55 and CH55 was slightly higher than that reaching 5.6 g/L. In contrast, the SCOD of PB70 and CH70 increased sharply up to 42.1 and 49.7 g/L. The hydrolysis efficiency was calculated based on these SCOD concentrations (Figure 1F and Table S4) and reached just 2.73 ± 0.08% and 2.83 ± 0.05% for PB35 and CH35 experiments. For PB55 and CH55, the hydrolysis efficiency was higher, reaching 5.86 ± 0.15% and 5.74 ± 0.12%, respectively. The fastest disintegration and hydrolysis processes occurred at 70 °C (Figure S1), leading to the highest hydrolysis efficiencies of 36.31 ± 0.56% (CH70) and 30.8 ± 0.02% (PB70) after 56 days. A complete hydrolysis of the entire TPS material was not observed. This could be due to the expected presence of carbon black materials, which are considered nonbiodegradable.[48]

From the hydrolysis experiments, it was also observed that the temperature significantly affected the pH of the produced hydrolysates. TPS mulch film typically contains several biopolymers, providing many plausible chemicals that could be formed after hydrolysis.[27,28] For example, PLA can be present and will be hydrolyzed into lactic acid, causing a significant drop in the pH of the medium as shown earlier.[49] The most intense pH decline was found at the highest applied temperature without buffer supply (experiment CH70) where the pH dropped from 6.13 to 3.02 within 10 days (Figure 1E). Hereafter, a further consistent decrease to pH 2.57 until day 56 was shown. A similar but more moderate trend can be found in CH55, CH35, and PB70. Here, pH dropped from neutral to 3.03, 4.82, and 3.58, respectively. PB35, as well as PB55, remained almost unchanged at pH 7 until the end of hydrolysis. As previously mentioned, the CH70 experiment reached the lowest measured pH, which interestingly coincided with the highest measured SCOD. The use of buffer had a noticeable effect as well, as experiments in a buffered medium consistently ended with a higher pH compared to those in demineralized water at each respective temperature.

The microplastic formation was studied for the experiments at 70 °C. Specific number-based and volume-based modal diameters were selected to analyze microplastic particle size distribution after hydrolysis, which is similar to earlier work.[50] Samples were taken at the end of the experiment (see Figure 1G,H) and showed that the highest number of particles had a particle diameter of 675 μm and represented 8.8% (PB70) and 13.0% (CH70). However, PB70 (35.5%) had a higher number of small particles (<294 μm) than CH70 (10.9%). The results of the volume-based modal diameter were similar to those of PB70, which had a smaller volume of plastic particles than CH70. Also, the water in PB70 became more turbid (as visible by the eye) than in CH70 (Figure 1C,D). Looking at the smallest particles, it was found that particles from sizes as small as 100 μm were detected. No particles were found in the range of 1200 μm up to 2500 μm. This was expected since the analyzed sample retrieved was first filtered over a 1 mm mesh to remove larger particles that may hinder the laser diffraction analysis. These results show that phosphate buffer affects microplastic formation during hydrolysis, which causes smaller than 300 μm microplastic formation. Further monitoring of plastic size dynamics and hydrolysate formation can reveal how the various particles are formed, providing solid understanding to control or reduce microplastic formation.

3.2. Residual TPS Analysis with XRD and FTIR Designates Removal of Starch and PLA. XRD analysis was conducted on the original TPS and on the hydrolyzed TPS mulch film leftover from a single hydrolysis experiment (selected from CH70). This allowed further investigation of the TPS composition changes during the degradation process. In Figure 2A, the XRD pattern depicts that the residual CH70 solid material has five distinct wide peaks at 16.1°, 17.3°, 20.4°, 23.0°, and 24.8°, which may correspond to PBAT polymer.[51,52] The characteristic peaks for starch appeared at 12.8° and 19.7°, similar to the previous study.[52] Additionally, the crystallinity ratio increased slightly from 13.1% to 21.4% after hydrolysis

https://doi.org/10.1021/acssuschemeng.5c02366
ACS Sustainable Chem. Eng. 2025, 13, 8116−8127

(Figure S2). This could mean that the amorphous components of TPS mulch film were (at least partly) hydrolyzed at 70 °C and indicate that the residues have an overall higher crystallinity that is typically more tough to degrade than amorphous components.[53] Meanwhile, Figure 2B presents the FTIR spectra of TPS before and after hydrolysis, reflecting changes in the polymer chemical structure caused by hydrolytic degradation. Compared with the standard FTIR spectra of PBAT, the original and hydrolyzed TPS mulch film showed similar feature absorption peaks at 1711 and 726 cm^{-1} (Figure 2B, orange area), which were attributed to the vibration of C═O and $[-C-H_2-]_n \geq 4$ in PBAT.[54] The FTIR absorption peaks at 3450−3300 cm^{-1} (Figure 2B, green area) were designated as the −OH hydroxyl stretch of the corn starch peak,[55] which can be seen to weaken as the starch from the TPS is likely hydrolyzed into sugars. Moreover, an absorption peak at 1080 cm^{-1} (Figure 2B, blue dashed line) was found, which may correspond to the functional group of the −C−O− stretch in PLA. After hydrolysis, this peak disappeared, further suggesting that PLA was removed from the TPS and hydrolysis of this polymer likely took place.

3.3. Hydrolysis of TPS Provides a Spectrum of Chemicals Derived from Different Polymers. The analysis of the hydrolysates revealed the formation of a spectrum of monomeric compounds and occasionally probable microbially produced biochemicals. Hydrolytic depolymerization of polymers is aligned with processes such as disintegration and hydrolysis.[53] This is typically accompanied by oligomer, monomer formation, and leaching of various additives.[56] To validate whether the TPS hydrolysates indeed contained potential upgradeable compounds, a composition analysis of hydrolysate was done. This analysis revealed that glucose, lactate, TPA, AA, and 1,4-BDO were found (Figure 3). In all experiments, the identified products could not explain all of the SCOD; a remarkable part remained unidentified. Plausible compounds were not determined that included TPS additives like glycerol or vegetable oils,[57] as well as possible oligomers.

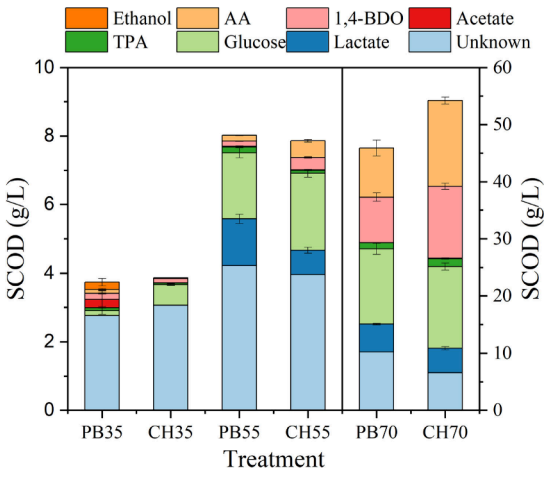

Figure 3. Detected chemicals were present in the liquid fraction of hydrolyzed TPS at day 56. Data are expressed in SCOD. PB35, PB55, and PB70 refer to experiments conducted with phosphate buffer solution and demineralized water as the medium at 35 °C, 55 °C, and 70 °C, respectively. CH35, CH55, and CH70 refer to experiments with only demineralized water in the medium at 35 °C, 55 °C, and 70 °C, respectively. Error bars represent the standard deviation.

The identified chemicals that were released upon hydrolysis could all be attributed to either originating from mulch film constituent polymers or microbial activity. Lactate could originate as a monomer from PLA, and the monomers of 1,4-BDO, TPA, and AA could originate from PBAT. These results further confirm the XRD and FTIR findings that indicate that the TPS mulch film contains PLA and PBAT. Glucose was found in each group because the glycosidic bond of starch can be hydrolyzed into sugars within aquatic environments.[46] However, no lactate was observed in PB35 and CH35; acetate and ethanol were surprisingly found, accounting for 6.3% and 5.8% of the SCOD, respectively, in PB35 (Figures 3 and S3). These chemicals are not known to be formed under chemical hydrolysis conditions but are known end-metabolites from anaerobic glucose fermentation.[58] So, the formation of acetate and ethanol suggests that microbes were active during hydrolysis, even without an exogenous nutrient supply besides phosphate. This microbial activity was supported via microscopic observations that showed distinct bacterial cells after hydrolysis completion (see Figure S4). The origin of these microorganisms could be in the lab environment. For microbial growth, nutrients are required, which could mean that nutrients were derived from the provided TPS. We speculate that the studied TPS mulch film contains nutrients, either remaining from the original biobased materials or intentionally added to promote end-of-life biodegradation in the field.

By comparing the pH of the experiments, it was found that PB35 remained almost neutral, while for CH35, the pH dropped to 4.8. In the experiments, the pH dropped typically faster to a lower value (in the range of 6.13 to 3.02) at higher applied temperatures, which may have hampered microbial activity as less optimal conditions were present to allow substantial growth during the short experimental time compared to other studies.[58] The pH drops align with mulch film being hydrolyzed into acidic monomers derived from PBAT and PLA. In previous studies, the hydrolysates of PLA-containing polymers exhibited a higher amount of released lactate in the nonbuffered media compared to the buffered media, because PLA hydrolysis begins with protonation and is followed by the addition of water and the breaking of the ester link.[59] In contrast, during this study, the lactate concentration in the buffered media (PB55 and PB70) showed the opposite trend compared to the nonbuffered media (CH55 and CH70), with 92% and 13% higher lactate levels, respectively (Figure 3 and Figure S3B).

The 70 °C thermophilic condition also accelerated PBAT hydrolysis. As mentioned, PBAT hydrolysis explains the formation of AA, 1,4-BDO, and TPA monomers. Notably, AA, 1,4-BDO, and AA concentrations at 35 and 55 °C were significantly lower than 70 °C (Figure 3 and Figure S3). The highest concentrations of AA, 1,4-BDO, and TPA reached 9.68, 5.90, and 0.86 g/L, respectively, in CH70 experiments. This could mean that temperature is one of the limiting factors in PBAT hydrolysis, and that higher than 55 °C would benefit PBAT hydrolysis. Deshoulles et al. reported that hydrolysis of PBAT occurs first on the ester group located between the terephthalate and adipate groups, leading to a decrease in molar mass.[60] Consequently, the ester bond between TPA and 1,4-BDO is tougher to hydrolyze than that between AA and 1,4-BDO, which is supported by a large amount of 1,4-BDO and AA release compared to the small amount of TPA release.

https://doi.org/10.1021/acssuschemeng.5c02366
ACS Sustainable Chem. Eng. 2025, 13, 8116−8127

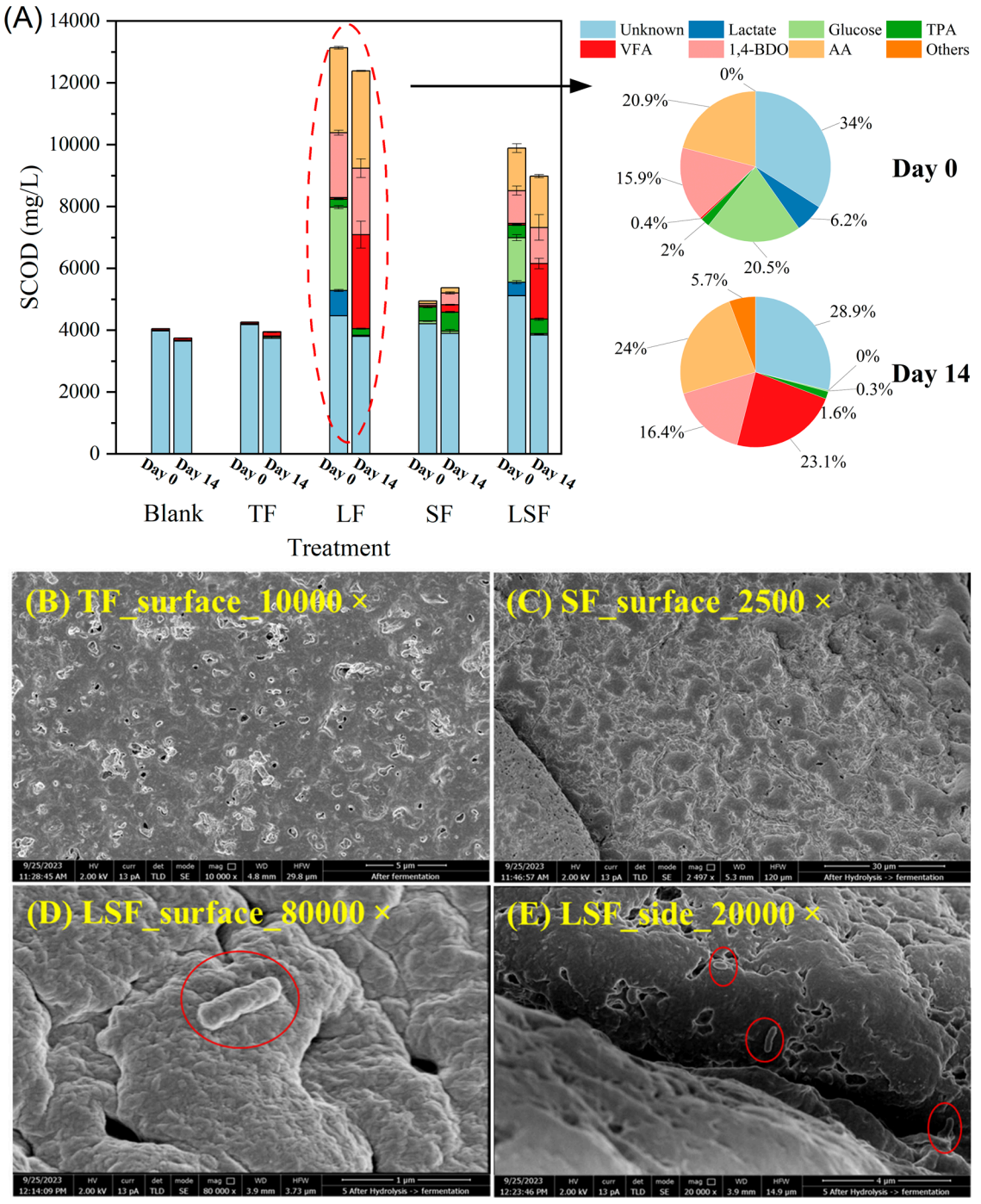

Figure 4. (A) Batch fermentation experiments of TPS and its hydrolysates: (i) original TPS fraction (TF) material, (ii) the liquid fraction (LF) of hydrolyzed TPS at 70 °C, (iii) the residual solid fraction (SF) of hydrolyzed TPS at 70 °C, and (iv) the combined hydrolyzed liquid and solid fraction (LSF) after hydrolysis. Chemical compounds identified in the fermentation broth are shown for days 0 and 14, based on soluble chemical oxygen demand (SCOD)."Unknown" refers to SCOD attributed to medium, inoculum components, and additives. "Others" refers to biomass. Error bars indicate the standard deviation. (B–E) SEM images of various fermented TPS mulch film residues (names given in image) at day 14; the red circles point out the featured microorganisms.

3.4. Anaerobic Fermentation of TPS and/or Its Hydrolysate Leads to Carboxylate Formation. The fermentation findings show that up to 5 different VFAs were produced from supplied TPS hydrolysates (derived from experiment CH70) or solid TPS. Glucose and lactate (derived from starch and PLA) were the likable intermediates responsible for this. To obtain these insights, anaerobic batch fermentations were conducted to explore the feasibility of converting (i) the original TPS fraction (TF) materials, (ii) the liquid fraction (LF) of hydrolyzed TPS, (iii) the residual solid fraction (SF) after hydrolysis, and (iv) the combination of liquid and solid fractions (LSF) after hydrolysis. Experiments were conducted at 35 °C, similar to the lowest temperature used for the hydrolysis experiments. With the application of a mixed-culture inoculum, a diverse portfolio of microbial conversions could occur due to the extensive

https://doi.org/10.1021/acssuschemeng.5c02366
ACS Sustainable Chem. Eng. 2025, 13, 8116−8127

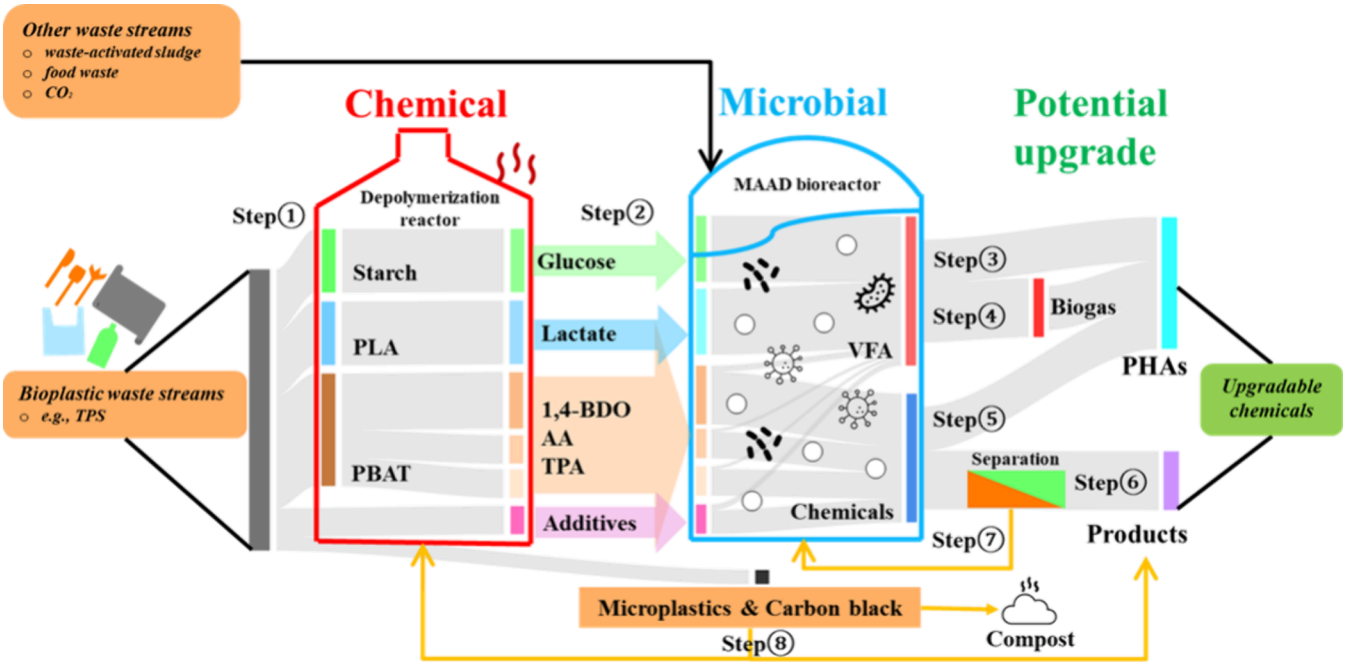

Figure 5. Biorefinery concept for mixed (containing TPS) biodegradable plastic waste streams recycled with microbial fermentation processes to produce a spectrum of upgradable chemicals. The steps 1−8 are explained in Section 3.5.

metabolic potential present in such consortia.[61] For instance, with the presence of glucose and lactate in the hydrolysates, it was expected that VFA such as acetate could be formed since this is a key intermediate in the anaerobic digestion of glucose or lactate into biogas.[62,63] With the supplemented methanogenic inhibitor, methane formation from acetate was suppressed, which could support the accumulation of acetate.[30]

Figure S4 shows that the supplied hydrolysates, containing the described spectrum of known and partly unknown compounds (see Section 3.3), were successfully converted to VFAs within 14 days. Acetate, propionate, and butyrate were the main VFAs found. The gas composition and pH changes reflected the microbial activities during fermentation. In all fermentation experiments, oxygen and methane remained below the quantification limit of 0.1 vol %, indicating anaerobic and arrested methanogenesis conditions.[30] In LF and LSF experiments, it was observed that the percentage of CO_2 increased, while N_2 decreased. Meanwhile, the pH dropped significantly from around 7 to 6.38 and 6.56 within 2 days, which can be explained by VFA production from neutral compounds such as glucose (Figure S6).[64] There was a distinct increase in the production of acetate, propionate, and *n*-butyrate within 5 days (Figure S6, LF and LSF). Meanwhile, ethanol, iso-butyrate, and iso-valerate were also detected at lower concentrations in this fermentation broth. Ethanol was produced during the first 2 days but then was quickly consumed (Figure S6D). Microbes can utilize acetate and propionate as electron acceptors and ethanol or lactate as electron donors to produce medium-chain fatty acids.[49,65] Likewise, the consumption of ethanol and lactate (e.g., from the supplied hydrolysate) and the formation of *n*-butyrate explain that the chain elongation bioprocess possibly happened during anaerobic fermentation. Albeit low, it was still notable that some acetate was formed from the solid TPS material (TF). This relatively low VFA production could match with earlier work, which reports that hydrolysis is considered a rate-limiting step in the microbial degradation of solid biodegradable plastics and thus limiting the formation of degradation products such as acetate or biogas.[17]

Figure 4A shows that glucose and lactate concentrations completely declined after fermentation in the LF and LSF experiments. Still, the monomers of PBAT, such as TPA, AA, and 1,4-BDO, were not (or not fully) anaerobically converted to VFAs (see Table S3). Abou-Zeid et al. reported that the PBAT polymer exhibits a low anaerobic microbial susceptibility.[66] Cazaudehore et al. reported that little or no anaerobic degradation occurred for PBAT at 38 °C.[67] However, this does not mean that PBAT monomers are not anaerobically fermentable. Xu et al. found that an upflow anaerobic sludge blanket (UASB) reactor showed excellent removal effects for 1,4-BDO.[68] Poulsen et al. utilized certain PBAT monomers as single carbon sources for thermophilic anaerobic digestion and proved that 1,4-BDO and AA were assimilated into biomass.[69] Li et al. found that TPA can be 100% degraded in a UASB reactor at 37 °C in 208 days.[70] Matthies et al. used sea sediments as inoculum and successfully converted AA into acetate, propionate, and methane.[71] This evidence suggests that monomers of PBAT are anaerobically digestible and have at least partial potential to be converted to VFA under the right conditions. The provided inoculum and liquid TPS fractions also contained 34.2% of unknown SCOD; these may also be of use to produce VFAs. For example, glycerol may be present in the hydrolysate, which also can be microbially converted into VFA.[72] Overall, the various experiments clearly showed that up to 5 different VFAs were formed, while glucose and lactate were completely consumed. The hydrolyzed TPS (LF) showed relatively high VFA production efficiency, in which 23.1% of the SCOD was converted into VFAs. With the TPS hydrolysis efficiency of 36.3% (see Section 3.1) found above, it was calculated that up to 10% of the original solid TPS material was converted into VFAs via the LF experiment.

After anaerobic fermentation of unhydrolyzed solid TPS (TF), the morphology of the fermented TPS exhibited many small holes on the surface (Figure 4B), which were likely

https://doi.org/10.1021/acssuschemeng.5c02366
ACS Sustainable Chem. Eng. 2025, 13, 8116−8127

caused by starch degradation. These results are similar to a previous starch-based plastic anaerobic digestion study.[73] For both TPS fermentation groups (SF and LSF), a clear net structure and irregular cracks were observed on the surface at the end of the experiment. Interestingly, shapes resembling bacteria were found on the surfaces of TPS residues (Figure 4D,E). Compared with the TF and SF groups, supplying more soluble substrates in the medium at the beginning of fermentation (LSF) could be a feasible strategy to enhance microbial growth. This may also stimulate exocellular enzyme secretion of bacteria, since more digestible carbon served as substrate (in this study, glucose and lactate), which could be beneficial for solid TPS hydrolysis and facilitate fermentation processes.

3.5. TPS Depolymerization and Anaerobic Fermentation Support Various Routes to Deliver Upgradable Chemicals. The presented work adds to the perspectives on recycling biodegradable plastics via microbial processes. As mentioned in the Introduction, whether it is, for example, to reduce environmental plastic pollution or to expand the market for biodegradable plastics, there is an urgent interest to establish a biodegradable plastic recycling strategy that is ideally compatible with current waste management systems.[74,75] The insights from this study support the development of a new biorefinery concept, including various routes to recycle mixed biodegradable plastic waste streams (Figure 5). TPS, and expectedly the starch and PLA content, can be effectively converted into VFA. The present study is the first one to utilize TPS material via mixed-culture anaerobic fermentation for applications beyond biogas production. Prior studies have already noted the importance of other biodegradable plastics (like PLA or PHA) recycling into VFAs via mixed-culture fermentation[43,49,76] (steps ① and ② in Figure 5). With the plurality of polymers and metabolic microbial capabilities, many biochemicals may be further recovered as discussed in present and other studies.[76] Still, mixed microbial cultures can also have certain boundaries, as not all materials present in plastic waste can be converted into VFAs or other upgradable chemicals. Materials based on polymers like polypropylene or polyethylene terephthalate may be better treatable via thermolysis processes.[3] In future studies, care should also be taken on the accumulation of potential microbial inhibiting compounds like TPA, which may limit certain fermentation processes.[69] The exploitation of mixed-microbial cultures provides potential ways to especially handle mixed plastic waste streams similar to those shown in industrial-scale biogas production plants.[21] In these digesters, various microorganisms live together, enabling a certain resilience and building syntrophic relations to funnel complex biomass-waste materials into methane-rich biogas. Similarly, the emerging amounts of biodegradable plastic products could be used at their end-of-life as substrates to feed-in anaerobic fermenters and produce VFA (or alternatively biogas) as well.[8] These VFA (or alternatively the methane) can be used for renewable PHA material production routes, allowing for value and material recovery from biodegradable plastic waste streams (steps ③ and ④ in Figure 5).[23,33] These plastic-derived feedstocks may even be mixed with other biowaste sources, such as waste-activated sludge, food waste, and CO_2 that also are used for VFA formation.[77] Hereby, microbial community analysis and understanding of the interactions will also be of value to further develop the microbial conversion processes of biodegradable plastic waste.

Meanwhile, the results of the anaerobic fermentation present here lead to a mix of partially identified chemicals. It is also interesting to develop separation and purification techniques to recover chemicals from such mixed streams (step ⑥ in Figure 5). Several findings contributed to this. Shen et al. reported a chemical method to recover AA and TPA from PBAT.[78] Parodi et al. found that, via selective solubilization and depolymerization of starch-based plastic, it is possible to recover 1,4-butanediol, dimethyl terephthalate, and dimethyl adipate.[79] However, care should be taken with regard to the presence of nutrients that may cause precipitation due to pH change during chemical recovery methods. In addition, the present study found 1,4-BDO, AA, and TPA also serve as potential substrates to produce PHA type bioplastic materials (step ⑤ in Figure 5). For example, Bao et al. reported that TPA was used as a carbon source for PHA production.[80] Zhang et al. reported the utilization of 1,4-BDO and glucose as carbon sources to produce PHA by engineered *Halomonas bluephagenesis*.[81] Moreover, AA can also be utilized as a single carbon source to produce PHA by *Pseudomonas putida*.[82] An open-culture PHA production approach could be followed to find suitable microorganisms that can deal with the specific mix of monomers for PHA formation.

However, not all TPS plastic was fermented in the present study, while solid residues remained after hydrolysis or anaerobic fermentation. Also, not all COD was identified, and additives that are likely present should also be dealt with. Even with the potential recovered spectrum of chemicals, waste streams can occur. Additionally, the hydrolysis and various fermentation processes also have to deal with the needed supply of water, chemicals (e.g., for pH control), and/or microbial nutrients. For this, suitable recycling steps should also be considered to close loops and reduce the external input needs (step ⑦ in Figure 5). Still, some parts that are difficult to convert at moderate conditions (like carbon black and microplastic) may still be concentrated and recoverable by settling processes; then, they can go back to the hydrolysis reactor or compost facility (step ⑧ in Figure 5). As the market and demand for biodegradable plastics grows, further research on the capabilities of microorganisms to utilize biodegradable plastic as feedstock is of value.[3,9] Hereby, the economic and environmental performance on comprehensive engineered routes should also be assessed to get more understanding of the actual applicability.

■ ASSOCIATED CONTENT

Data Availability Statement

The original data presented in this paper is available at the 4TU.Research Database: https://doi.org/10.4121/4112fbf6-44cd-4f07-a0e1-0843c8e6ba35.

Supporting Information

The Supporting Information is available free of charge at https://pubs.acs.org/doi/10.1021/acssuschemeng.5c02366.

The composition of the microbial nutrient medium for anaerobic fermentation experiments (Table S1), the weight loss of TPS mulch film after hydrolysis at 70 °C (Table S2), the concentration of identified TPS mulch film monomers before and after fermentation (Table S3), the hydrolysis efficiency of TPS mulch film at day 56 and VFA yield before and after fermentation (Table S4), the track of TPS disintegration and hydrolysis processes within 56 days (Figure S1), the crystallinity

https://doi.org/10.1021/acssuschemeng.5c02366
ACS Sustainable Chem. Eng. 2025, 13, 8116−8127

degree of the TPS mulch film and hydrolyzed TPS at 70 °C at day 56 (Figure S2), the monomer concentration of TPS hydrolysate at day 56 (Figure S3), light microscope image of TPS hydrolysate at day 56 (Figure S4), the pH, headspace pressure, and gas composition of fermentation experiments (Figure S5), and the VFA and ethanol concentration of fermentation experiments (Figure S6) (PDF)

AUTHOR INFORMATION

Corresponding Author

David P. B. T. B. Strik − *Environmental Technology, Wageningen University and Research, Wageningen 6708 WG, The Netherlands;* orcid.org/0000-0003-0591-682X; Email: david.strik@wur.nl

Authors

Weishen Zeng − *Environmental Technology, Wageningen University and Research, Wageningen 6708 WG, The Netherlands*

Kasper D. de Leeuw − *Environmental Technology, Wageningen University and Research, Wageningen 6708 WG, The Netherlands;* orcid.org/0000-0001-8145-2604

Complete contact information is available at: https://pubs.acs.org/10.1021/acssuschemeng.5c02366

Author Contributions

W.Z. contributed to the experimental design, data acquisition, analysis, interpretation, and drafting of the original manuscript. K.D.d.L. provided support for data analysis, manuscript revision, and project supervision. D.P.B.T.B.S. conceived the project and contributed to data analysis, manuscript review, editing, and overall project supervision. All authors have read and approved the final manuscript.

Notes

D.P.B.T.B.S. is an employee of Wageningen University & Research (WUR) fulfilling the role of one of the platform managers of Unlock (https://m-unlock.com). K.D.d.L. is a lecturer at WUR as well as senior researcher at ChainCraft (https://chaincraft.com).

The authors declare no competing financial interest.

ACKNOWLEDGMENTS

This work was supported by a grant from the China Scholarship Council (CSC, 202208440013) and Biotech Booster (https://www.biotechbooster.nl/projects/biocircular-plastic-initiative/). We would like to thank Lucian Wester, Beatriz Alvarado Perry, and Katja Grolle for their expertise in helping with the monomers analysis of the TPS mulch film. We also thank Ilse Gerrits and Wouter Teunissen for helping with XRD and FTIR measurements.

ABBREVIATIONS

MAAD, methane-arrested anaerobic digestion; VFAs, volatile fatty acids; MCFAs, medium-chain fatty acids; PLA, polylactic acid; TPS, thermoplastic starch; PHAs, polyhydroxyalkanoates; PBAT, poly(butylene adipate-*co*-terephthalate); AA, adipic acid; 1,4-BDO, 1,4-butanediol; TPA, terephthalic acid; BrES, 2-bromoethanesulfonate; PBS, phosphate buffer solution

REFERENCES

(1) Nielsen, T. D.; Hasselbalch, J.; Holmberg, K.; Stripple, J. Politics and the plastic crisis: A review throughout the plastic life cycle. *WIREs Energy and Environment* **2020**, *9* (1), e360.

(2) Vidal, F.; van der Marel, E. R.; Kerr, R. W. F.; McElroy, C.; Schroeder, N.; Mitchell, C.; Rosetto, G.; Chen, T. T. D.; Bailey, R. M.; Hepburn, C.; et al. Designing a circular carbon and plastics economy for a sustainable future. *Nature* **2024**, *626* (7997), 45−57.

(3) Rosenboom, J. G.; Langer, R.; Traverso, G. Bioplastics for a circular economy. *Nat. Rev. Mater.* **2022**, *7* (2), 117−137.

(4) European Commission. *A European Strategy for Plastics in a Circular Economy*; https://eur-lex.europa.eu/legal-content/EN/TXT/?qid=1516265440535&uri=COM:2018:28:FIN (accessed 2024 September 9).

(5) United Nations. *UN Plastics Treaty*; https://www.globalplasticlaws.org/un-global-plastics-treaty (accessed 2025 January 10).

(6) Yu, Y.; Flury, M. Unlocking the Potentials of Biodegradable Plastics with Proper Management and Evaluation at Environmentally Relevant Concentrations. *npj Materials Sustainability* **2024**, *2* (1), 9.

(7) Chen, G. Y.; Li, J. Y.; Sun, Y. N.; Wang, Z.; Leeke, G. A.; Moretti, C.; Cheng, Z. J.; Wang, Y.; Li, N.; Mu, L.; et al. Replacing Traditional Plastics with Biodegradable Plastics: Impact on Carbon Emissions. *Engineering-Prc* **2024**, *32*, 152−162.

(8) Narancic, T.; Verstichel, S.; Reddy Chaganti, S.; Morales-Gamez, L.; Kenny, S. T.; De Wilde, B.; Babu Padamati, R.; O'Connor, K. E. Biodegradable Plastic Blends Create New Possibilities for End-of-Life Management of Plastics but They Are Not a Panacea for Plastic Pollution. *Environ. Sci. Technol.* **2018**, *52* (18), 10441−10452.

(9) Europeanbioplastics. https://www.european-bioplastics.org/bioplastics-market-development-update-2024/# (accessed 2025 January 10).

(10) Brodhagen, M.; Peyron, M.; Miles, C.; Inglis, D. A. Biodegradable plastic agricultural mulches and key features of microbial degradation. *Appl. Microbiol. Biotechnol.* **2015**, *99* (3), 1039−1056.

(11) Molenveld, K.; Bos, H.; van der Spa, M. *Biobased Plastics 2020*; Wageningen Food & Biobased Research, 2020; https://edepot.wur.nl/534587.

(12) Shah, F.; Wu, W. Use of plastic mulch in agriculture and strategies to mitigate the associated environmental concerns. *Adv. Agron* **2020**, *164*, 231−287.

(13) Europeanbioplastics. https://www.european-bioplastics.org/faq-items/how-much-agricultural-area-is-used-for-bioplastics/ (accessed 2024 September 9).

(14) van den Oever, M.; Molenveld, K.; van der Zee, M.; Bos, H. *Bio-based and biodegradable plastics: Facts and Figures: Focus on food packaging in the Netherlands*; Wageningen Food & Biobased Research, 2017; DOI: 10.18174/408350.

(15) Atiwesh, G.; Mikhael, A.; Parrish, C. C.; Banoub, J.; Le, T. T. Environmental impact of Bioplastic use: A review. *Heliyon* **2021**, *7* (9), No. e07918.

(16) Ballerstedt, H.; Tiso, T.; Wierckx, N.; Wei, R.; Averous, L.; Bornscheuer, U.; O'Connor, K.; Floehr, T.; Jupke, A.; Klankermayer, J.; et al. MIXed plastics biodegradation and UPcycling using microbial communities: EU Horizon 2020 project MIX-UP started January 2020. *Environ. Sci. Eur.* **2021**, *33* (1), 99.

(17) Cazaudehore, G.; Guyoneaud, R.; Evon, P.; Martin-Closas, L.; Pelacho, A. M.; Raynaud, C.; Monlau, F. Can. anaerobic digestion be a suitable end-of-life scenario for biodegradable plastics? A critical review of the current situation, hurdles, and challenges. *Biotechnol Adv.* **2022**, *56*, No. 107916.

(18) Ellis, L. D.; Rorrer, N. A.; Sullivan, K. P.; Otto, M.; McGeehan, J. E.; Román-Leshkov, Y.; Wierckx, N.; Beckham, G. T. Chemical and biological catalysis for plastics recycling and upcycling. *Nature Catalysis* **2021**, *4* (7), 539−556.

(19) Gercke, D.; Furtmann, C.; Tozakidis, I. E. P.; Jose, J. Highly Crystalline Post-Consumer PET Waste Hydrolysis by Surface

Displayed PETase Using a Bacterial Whole-Cell Biocatalyst. *ChemCatChem.* **2021**, *13* (15), 3479−3489.
(20) Zeeman, G.; Lettinga, G. The role of anaerobic digestion of domestic sewage in closing the water and nutrient cycle at community level. *Water Sci. Technol.* **1999**, *39* (5), 187−194.
(21) World Biogas Association. https://www.worldbiogasassociation.org/wp-content/uploads/2019/07/WBA-globalreport-56ppa4_digital.pdf (accessed 2024 September 9).
(22) Mango. https://www.mangomaterials.com/innovation/ (accessed 2024 September 9).
(23) López, J. C.; Arnáiz, E.; Merchán, L.; Lebrero, R.; Muñoz, R. Biogas-based polyhydroxyalkanoates production by Methylocystis hirsuta: A step further in anaerobic digestion biorefineries. *Chem. Eng. J.* **2018**, *333*, 529−536.
(24) *BIOPLAST*; https://omnexus.specialchem.com/product/t-biotec-bioplast-tps (accessed 2024 September 9).
(25) Agarwal, S. Major factors affecting the characteristics of starch based biopolymer films. *Eur. Polym. J.* **2021**, *160*, 110788.
(26) Surendren, A.; Mohanty, A. K.; Liu, Q.; Misra, M. A review of biodegradable thermoplastic starches, their blends and composites: recent developments and opportunities for single-use plastic packaging alternatives. *Green Chem.* **2022**, *24* (22), 8606−8636.
(27) Paola Bracciale, M.; De Gioannis, G.; Falzarano, M.; Muntoni, A.; Polettini, A.; Pomi, R.; Rossi, A.; Sarasini, F.; Tirillò, J.; Zonfa, T. Disposable Mater-Bi Bioplastic tableware: Characterization and assessment of anaerobic biodegradability. *Fuel* **2024**, *355*, 129361.
(28) Bastioli, C. Properties and applications of Mater-Bi starch-based materials. *Polym. Degrad. Stab.* **1998**, *59* (1−3), 263−272.
(29) Olokede, O.; Liu, K.; Holtzapple, M. The Impact of Preservation Techniques on Methane-Arrested Anaerobic Digestion of Nutrient-Rich Feedstocks. *Appl. Biochem. Biotechnol.* **2023**, *195* (1), 331−352.
(30) Wu, H.; Dalke, R.; Mai, J.; Holtzapple, M.; Urgun-Demirtas, M. Arrested methanogenesis digestion of high-strength cheese whey and brewery wastewater with carboxylic acid production. *Bioresour. Technol.* **2021**, *332*, No. 125044.
(31) Darwin; Cord-Ruwisch, R.; Charles, W. Ethanol and lactic acid production from sugar and starch wastes by anaerobic acidification. *Eng. Life Sci.* **2018**, *18* (9), 635−642.
(32) de Leeuw, K. D.; Ahrens, T.; Buisman, C. J. N.; Strik, D. Open Culture Ethanol-Based Chain Elongation to Form Medium Chain Branched Carboxylates and Alcohols. *Front Bioeng Biotechnol* **2021**, *9*, No. 697439.
(33) Perez-Zabaleta, M.; Atasoy, M.; Khatami, K.; Eriksson, E.; Cetecioglu, Z. Bio-based conversion of volatile fatty acids from waste streams to polyhydroxyalkanoates using mixed microbial cultures. *Bioresour. Technol.* **2021**, *323*, No. 124604.
(34) Agler, M. T.; Wrenn, B. A.; Zinder, S. H.; Angenent, L. T. Waste to bioproduct conversion with undefined mixed cultures: the carboxylate platform. *Trends Biotechnol* **2011**, *29* (2), 70−78.
(35) STOCKER. *Bio Mulch Folie*. https://demoestuinwinkel.nl/products/mulch-folie-biologisch-afbreekbaar?variant=42078102454515&currency=EUR&utm_medium=product_sync&utm_source=google&utm_content=sag_organic&utm_campaign=Shopify_feed&srsltid=AfmBOopqmMKBQKYaoGVtTlNLn9IJFzIKa8YsVfyi1z86bQFpyznADKSyQEs (accessed 2023 March 6).
(36) NOVAMONT. *Pacciamatura biodegradabile compostabile*; https://materbi.com/wp-content/uploads/2023/12/pacciamatura_IT_LR_09.2019.pdf (accessed 2023 March 6).
(37) NOVAMONT. *Mater-Bi*; https://www.novamont.com/eng/mater-bi (accessed 2023 March 6).
(38) de Leeuw, K. D.; Buisman, C. J. N.; Strik, D. Branched Medium Chain Fatty Acids: Iso-Caproate Formation from Iso-Butyrate Broadens the Product Spectrum for Microbial Chain Elongation. *Environ. Sci. Technol.* **2019**, *53* (13), 7704−7713.
(39) Zhou, Z.; Meng, Q.; Yu, Z. Effects of methanogenic inhibitors on methane production and abundances of methanogens and cellulolytic bacteria in in vitro ruminal cultures. *Appl. Environ. Microb* **2011**, *77* (8), 2634−2639.
(40) Rodriguez-Gonzalez, F. J.; Ramsay, B. A.; Favis, B. D. High performance LDPE/thermoplastic starch blends: a sustainable alternative to pure polyethylene. *Polymer* **2003**, *44* (5), 1517−1526.
(41) Gong, M.; Yang, G.; Zhuang, L.; Zeng, E. Y. Microbial biofilm formation and community structure on low-density polyethylene microparticles in lake water microcosms. *Environ. Pollut.* **2019**, *252* (Pt A), 94−102.
(42) Yang, W.; Liu, R.; Li, C.; Song, Y.; Hu, C. Hydrolysis of waste polyethylene terephthalate catalyzed by easily recyclable terephthalic acid. *Waste Manag* **2021**, *135*, 267−274.
(43) Jin, Y.; de Leeuw, K. D.; Strik, D. Microbial Recycling of Bioplastics via Mixed-Culture Fermentation of Hydrolyzed Polyhydroxyalkanoates into Carboxylates. *Materials (Basel)* **2023**, *16* (7), 2693.
(44) Tyagi, P.; Agate, S.; Velev, O. D.; Lucia, L.; Pal, L. A Critical Review of the Performance and Soil Biodegradability Profiles of Biobased Natural and Chemically Synthesized Polymers in Industrial Applications. *Environ. Sci. Technol.* **2022**, *56* (4), 2071−2095.
(45) Griffin-LaHue, D.; Ghimire, S.; Yu, Y.; Scheenstra, E. J.; Miles, C. A.; Flury, M. In-field degradation of soil-biodegradable plastic mulch films in a Mediterranean climate. *Sci. Total Environ.* **2022**, *806* (Pt 1), No. 150238.
(46) Sander, M. Biodegradation of Polymeric Mulch Films in Agricultural Soils: Concepts, Knowledge Gaps, and Future Research Directions. *Environ. Sci. Technol.* **2019**, *53* (5), 2304−2315.
(47) Mina Hernandez, J. H. Effect of the Incorporation of Polycaprolactone (PCL) on the Retrogradation of Binary Blends with Cassava Thermoplastic Starch (TPS). *Polymers (Basel)* **2021**, *13* (1), 38.
(48) Sintim, H. Y.; Bary, A. I.; Hayes, D. G.; English, M. E.; Schaeffer, S. M.; Miles, C. A.; Zelenyuk, A.; Suski, K.; Flury, M. Release of micro- and nanoparticles from biodegradable plastic during in situ composting. *Sci. Total Environ.* **2019**, *675*, 686−693.
(49) Strik, D.; Heusschen, B. Microbial Recycling of Polylactic Acid Food Packaging Waste into Carboxylates via Hydrolysis and Mixed-Culture Fermentation. *Microorganisms* **2023**, *11* (8), 2103.
(50) Fang, Z.; Sallach, J. B.; Hodson, M. E. Ethanol, not water, should be used as the dispersant when measuring microplastic particle size distribution by laser diffraction. *Sci. Total Environ.* **2023**, *902*, No. 166129.
(51) Nomadolo, N.; Dada, O. E.; Swanepoel, A.; Mokhena, T.; Muniyasamy, S. A Comparative Study on the Aerobic Biodegradation of the Biopolymer Blends of Poly(butylene succinate), Poly(butylene adipate terephthalate) and Poly(lactic acid). *Polymers (Basel)* **2022**, *14* (9), 1894.
(52) Yokesahachart, C.; Yoksan, R.; Khanoonkon, N.; Mohanty, A. K.; Misra, M. Effect of jute fibers on morphological characteristics and properties of thermoplastic starch/biodegradable polyester blend. *Cellulose* **2021**, *28* (9), 5513−5530.
(53) Zhang, K.; Hamidian, A. H.; Tubic, A.; Zhang, Y.; Fang, J. K. H.; Wu, C.; Lam, P. K. S. Understanding plastic degradation and microplastic formation in the environment: A review. *Environ. Pollut.* **2021**, *274*, No. 116554.
(54) Ruggero, F.; Carretti, E.; Gori, R.; Lotti, T.; Lubello, C. Monitoring of degradation of starch-based biopolymer film under different composting conditions, using TGA, FTIR and SEM analysis. *Chemosphere* **2020**, *246*, No. 125770.
(55) Mendes, J. F.; Paschoalin, R. T.; Carmona, V. B.; Sena Neto, A. R.; Marques, A. C. P.; Marconcini, J. M.; Mattoso, L. H. C.; Medeiros, E. S.; Oliveira, J. E. Biodegradable polymer blends based on corn starch and thermoplastic chitosan processed by extrusion. *Carbohydr. Polym.* **2016**, *137*, 452−458.
(56) Kwan, C. S.; Takada, H. Release of Additives and Monomers from Plastic Wastes. In *Hazardous Chemicals Associated with Plastics in the Marine Environment, The Handbook of Environmental Chemistry*; Springer International Publishing, 2016; pp 51−70.

https://doi.org/10.1021/acssuschemeng.5c02366
ACS Sustainable Chem. Eng. 2025, 13, 8116−8127

(57) NOVAMONT. https://northamerica.novamont.com/public/Documentation/Bioplastics_crops.pdf (accessed 2023 March 6).
(58) Tamis, J.; Joosse, B.; de Leeuw, K.; Kleerebezem, R. High-rate ethanol production at low pH using the anaerobic granular sludge process. *Biotechnol. Bioeng.* **2021**, *118* (5), 1943−1950.
(59) Araque-Monrós, M. C.; Vidaurre, A.; Gil-Santos, L.; Gironés Bernabé, S.; Monleón-Pradas, M.; Más-Estellés, J. Study of the degradation of a new PLA braided biomaterial in buffer phosphate saline, basic and acid media, intended for the regeneration of tendons and ligaments. *Polym. Degrad. Stab.* **2013**, *98* (9), 1563−1570.
(60) Deshoulles, Q.; Le Gall, M.; Benali, S.; Raquez, J. M.; Dreanno, C.; Arhant, M.; Priour, D.; Cerantola, S.; Stoclet, G.; Le Gac, P. Y. Hydrolytic degradation of biodegradable poly(butylene adipate-co-terephthalate) (PBAT) - Towards an understanding of microplastics fragmentation. *Polym. Degrad. Stab.* **2022**, *205*, No. 110122.
(61) Bhatia, S. K.; Bhatia, R. K.; Choi, Y. K.; Kan, E.; Kim, Y. G.; Yang, Y. H. Biotechnological potential of microbial consortia and future perspectives. *Crit Rev. Biotechnol* **2018**, *38* (8), 1209−1229.
(62) Gao, C.; Doloman, A.; Alaux, E.; Rijnaarts, H. H. M.; Sousa, D. Z.; Hendrickx, T. L. G.; Temmink, H.; Sudmalis, D. De novo anaerobic granulation with varying organic substrates: granule growth and microbial community responses. *Sci. Total Environ.* **2024**, *951*, No. 175570.
(63) Satpathy, P.; Biernacki, P.; Cypionka, H.; Steinigeweg, S. Modelling anaerobic digestion in an industrial biogas digester: Application of lactate-including ADM1 model (Part II). *J. Environ. Sci. Health A Tox Hazard Subst Environ. Eng.* **2016**, *51* (14), 1226−1232.
(64) Elefsiniotis, P.; Wareham, D. G.; Smith, M. O. Effect of a starch-rich industrial wastewater on the acid-phase anaerobic digestion process. *Water Environ. Res.* **2005**, *77* (4), 366−371.
(65) Roghair, M.; Hoogstad, T.; Strik, D.; Plugge, C. M.; Timmers, P. H. A.; Weusthuis, R. A.; Bruins, M. E.; Buisman, C. J. N. Controlling Ethanol Use in Chain Elongation by CO(2) Loading Rate. *Environ. Sci. Technol.* **2018**, *52* (3), 1496−1505.
(66) Abou-Zeid, D. M.; Muller, R. J.; Deckwer, W. D. Biodegradation of aliphatic homopolyesters and aliphatic-aromatic copolyesters by anaerobic microorganisms. *Biomacromolecules* **2004**, *5* (5), 1687−1697.
(67) Cazaudehore, G.; Monlau, F.; Gassie, C.; Lallement, A.; Guyoneaud, R. Active microbial communities during biodegradation of biodegradable plastics by mesophilic and thermophilic anaerobic digestion. *J. Hazard Mater.* **2023**, *443* (Pt A), No. 130208.
(68) Xu, L.; Wang, Y.; Xuan, L.; Mei, H.; He, C.; Yang, J.; Wang, W. New attempts on acidic anaerobic digestion of poly (butylene adipate-co-terephthalate) wastewater in upflow anaerobic sludge blanket reactor. *J. Hazard Mater.* **2024**, *461*, No. 132586.
(69) Poulsen, J. S.; Trueba-Santiso, A.; Lema, J. M.; Echers, S. G.; Wimmer, R.; Nielsen, J. L. Assessing labelled carbon assimilation from poly butylene adipate-co-terephthalate (PBAT) monomers during thermophilic anaerobic digestion. *Bioresour. Technol.* **2023**, *385*, No. 129430.
(70) Li, H.; Zhang, W. D.; Xia, D.; Ye, L. F.; Ma, W. D.; Li, H. Y.; Li, Q. B.; Wang, Y. P. Improved anaerobic degradation of purified terephthalic acid wastewater by adding nanoparticles or co-substrates to facilitate the electron transfer process. *Environ. Sci-Nano* **2022**, *9* (3), 1011−1024.
(71) Matthies, C.; Schink, B. Anaerobic Degradation of Long-Chain Dicarboxylic-Acids by Methanogenic Enrichment Cultures. *Fems Microbiol Lett.* **1993**, *111* (2−3), 177−182.
(72) Leng, L.; Nobu, M. K.; Narihiro, T.; Yang, P.; Amy Tan, G. Y.; Lee, P. H. Shaping microbial consortia in coupling glycerol fermentation and carboxylate chain elongation for Co-production of 1,3-propanediol and caproate: Pathways and mechanisms. *Water Res.* **2019**, *148*, 281−291.
(73) Cucina, M.; De Nisi, P.; Trombino, L.; Tambone, F.; Adani, F. Degradation of bioplastics in organic waste by mesophilic anaerobic digestion, composting and soil incubation. *Waste Manag* **2021**, *134*, 67−77.
(74) Choi, S. Y.; Lee, Y.; Yu, H. E.; Cho, I. J.; Kang, M.; Lee, S. Y. Sustainable production and degradation of plastics using microbes. *Nat. Microbiol* **2023**, *8* (12), 2253−2276.
(75) Hinton, Z. R.; Talley, M. R.; Kots, P. A.; Le, A. V.; Zhang, T.; Mackay, M. E.; Kunjapur, A. M.; Bai, P.; Vlachos, D. G.; Watson, M. P.; et al. Innovations Toward the Valorization of Plastics Waste. *Annu. Rev. Mater. Res.* **2022**, *52* (1), 249−280.
(76) Garcia-Depraect, O.; Lebrero, R.; Rodriguez-Vega, S.; Borner, R. A.; Borner, T.; Munoz, R. Production of volatile fatty acids (VFAs) from five commercial bioplastics via acidogenic fermentation. *Bioresour. Technol.* **2022**, *360*, No. 127655.
(77) de Leeuw, K. D.; van Willigen, M. J. W.; Vrauwdeunt, T.; Strik, D. CO(2) supply is a powerful tool to control homoacetogenesis, chain elongation and solventogenesis in ethanol and carboxylate fed reactor microbiomes. *Front Bioeng Biotechnol* **2024**, *12*, No. 1329288.
(78) Shen, C. F.; Zhao, X.; Long, Y. W.; An, W. L.; Zhou, X. L.; Liu, X. H.; Xu, S. M.; Wang, Y. Z. Approach for the Low Carbon Footprint of Biodegradable Plastic PBAT: Complete Recovery of Its Every Monomer via High-Efficiency Hydrolysis and Separation. *Acs Sustainable Chemistry & Engineering* **2023**, *11* (5), 2005−2013.
(79) Parodi, A.; Arpaia, V.; Samorì, C.; Mazzocchetti, L.; Galletti, P. Novel Strategies for Recycling Poly(butylene adipate-coterephthalate)-Starch-Based Plastics: Selective Solubilization and Depolymerization−Repolymerization Processes. *Acs Sustainable Chemistry & Engineering* **2023**, *11* (39), 14518−14527.
(80) Bao, T.; Qian, Y.; Xin, Y.; Collins, J. J.; Lu, T. Engineering microbial division of labor for plastic upcycling. *Nat. Commun.* **2023**, *14* (1), 5712.
(81) Zhang, L.; Ye, J. W.; Zhang, X.; Huang, W.; Zhang, Z.; Lin, Y.; Zhang, G.; Wu, F.; Wang, Z.; Wu, Q.; et al. Effective production of Poly(3-hydroxybutyrate-co-4-hydroxybutyrate) by engineered Halomonas bluephagenesis grown on glucose and 1,4-Butanediol. *Bioresour. Technol.* **2022**, *355*, No. 127270.
(82) Ackermann, Y. S.; Li, W. J.; Op de Hipt, L.; Niehoff, P. J.; Casey, W.; Polen, T.; Kobbing, S.; Ballerstedt, H.; Wynands, B.; O'Connor, K.; et al. Engineering adipic acid metabolism in Pseudomonas putida. *Metab Eng.* **2021**, *67*, 29−40.

https://doi.org/10.1021/acssuschemeng.5c02366
ACS Sustainable Chem. Eng. 2025, 13, 8116−8127